Holographic optical tweezers combined with back-focal-plane displacement detection

Ferran Marsà,[1,3] Arnau Farré,[1,3] Estela Martín-Badosa,[1,2] and Mario Montes-Usategui[1,2,*]

[1]*Optical Trapping Lab – Grup de Biofotònica, Departament de Física Aplicada i Òptica, Universitat de Barcelona, Martí i Franquès 1, Barcelona 08028, Spain*

[2]*Institut de Nanociència i Nanotecnologia (IN2UB), Universitat de Barcelona, Martí i Franquès 1, Barcelona 08028, Spain*

[3]*These authors contributed equally to this work*

http://biopt.ub.edu

[*]*mario_montes@ub.edu*

Abstract: A major problem with holographic optical tweezers (HOTs) is their incompatibility with laser-based position detection methods, such as back-focal-plane interferometry (BFPI). The alternatives generally used with HOTs, like high-speed video tracking, do not offer the same spatial and temporal bandwidths. This has limited the use of this technique in precise quantitative experiments. In this paper, we present an optical trap design that combines digital holography and back-focal-plane displacement detection. We show that, with a particularly simple setup, it is possible to generate a set of multiple holographic traps and an additional static non-holographic trap with orthogonal polarizations and that they can be, therefore, easily separated for measuring positions and forces with the high positional and temporal resolutions of laser-based detection. We prove that measurements from both polarizations contain less than 1% crosstalk and that traps in our setup are harmonic within the typical range. We further tested the instrument in a DNA stretching experiment and we discuss an interesting property of this configuration: the small drift of the differential signal between traps.

OCIS codes: (140.7010) Laser trapping; (170.4520) Optical confinement and manipulation; (230.6120) Spatial light modulators; (350.4855) Optical tweezers or optical manipulation.

References and links

1. A. Ashkin, "Acceleration and trapping of particles by radiation pressure," Phys. Rev. Lett. **24**(4), 156–159 (1970).
2. D. G. Grier, "A revolution in optical manipulation," Nature **424**(6950), 810–816 (2003).
3. L. Nugent-Glandorf and T. T. Perkins, "Measuring 0.1-nm motion in 1 ms in an optical microscope with differential back-focal-plane detection," Opt. Lett. **29**(22), 2611–2613 (2004).
4. E. A. Abbondanzieri, W. J. Greenleaf, J. W. Shaevitz, R. Landick, and S. M. Block, "Direct observation of base-pair stepping by RNA polymerase," Nature **438**(7067), 460–465 (2005).
5. J. R. Moffitt, Y. R. Chemla, D. Izhaky, and C. Bustamante, "Differential detection of dual traps improves the spatial resolution of optical tweezers," Proc. Natl. Acad. Sci. U.S.A. **103**(24), 9006–9011 (2006).
6. K. Visscher, S. P. Gross, and S. M. Block, "Construction of multiple-beam optical traps with nanometer-resolution position sensing," IEEE J. Sel. Top. Quantum Electron. **2**(4), 1066–1076 (1996).
7. K. Sasaki, M. Koshioka, H. Misawa, N. Kitamura, and H. Masuhara, "Laser-scanning micromanipulation and spatial patterning of fine particles," Jpn. J. Appl. Phys. **30**(Part 2, No. 5B), L907–L909 (1991).
8. M. Capitanio, R. Cicchi, and F. S. Pavone, "Continuous and time-shared multiple optical tweezers for the study of single motor proteins," Opt. Lasers Eng. **45**(4), 450–457 (2007).
9. Y. Hayasaki, M. Itoh, T. Yatagai, and N. Nishida, "Nonmechanical optical manipulation of microparticle using spatial light modulator," Opt. Rev. **6**(1), 24–27 (1999).
10. https://sites.google.com/site/opticaltrappingpark/home/statistics
11. F. Belloni, S. Monneret, F. Monduc, and M. Scordia, "Multiple holographic optical tweezers parallel calibration with optical potential well characterization," Opt. Express **16**(12), 9011–9020 (2008).
12. A. van der Horst and N. R. Forde, "Calibration of dynamic holographic optical tweezers for force measurements on biomaterials," Opt. Express **16**(25), 20987–21003 (2008).

#198832 - $15.00 USD Received 4 Oct 2013; revised 19 Nov 2013; accepted 19 Nov 2013; published 3 Dec 2013

13. A. Farré, A. van der Horst, G. A. Blab, B. P. B. Downing, and N. R. Forde, "Stretching single DNA molecules to demonstrate high-force capabilities of holographic optical tweezers," J Biophotonics **3**(4), 224–233 (2010).
14. A. Farré, M. Shayegan, C. López-Quesada, G. A. Blab, M. Montes-Usategui, N. R. Forde, and E. Martín-Badosa, "Positional stability of holographic optical traps," Opt. Express **19**(22), 21370–21384 (2011).
15. C. H. J. Schmitz, J. P. Spatz, and J. E. Curtis, "High-precision steering of multiple holographic optical traps," Opt. Express **13**(21), 8678–8685 (2005).
16. M. Persson, D. Engström, A. Frank, J. Backsten, J. Bengtsson, and M. Goksör, "Minimizing intensity fluctuations in dynamic holographic optical tweezers by restricted phase change," Opt. Express **18**(11), 11250–11263 (2010).
17. G. Thalhammer, R. W. Bowman, G. D. Love, M. J. Padgett, and M. Ritsch-Marte, "Speeding up liquid crystal SLMs using overdrive with phase change reduction," Opt. Express **21**(2), 1779–1797 (2013).
18. R. Di Leonardo, F. Ianni, and G. Ruocco, "Computer generation of optimal holograms for optical trap arrays," Opt. Express **15**(4), 1913–1922 (2007).
19. M. Reicherter, T. Haist, E. U. Wagemann, and H. J. Tiziani, "Optical particle trapping with computer-generated holograms written on a liquid-crystal display," Opt. Lett. **24**(9), 608–610 (1999).
20. M. Montes-Usategui, E. Pleguezuelos, J. Andilla, and E. Martín-Badosa, "Fast generation of holographic optical tweezers by random mask encoding of Fourier components," Opt. Express **14**(6), 2101–2107 (2006).
21. S. Bianchi and R. Di Leonardo, "Real-time optical micro-manipulation using optimized holograms generated on the GPU," Comput. Phys. Commun. **181**(8), 1444–1448 (2010).
22. J. R. Moffitt, Y. R. Chemla, S. B. Smith, and C. Bustamante, "Recent advances in optical tweezers," Annu. Rev. Biochem. **77**(1), 205–228 (2008).
23. F. Gittes and C. F. Schmidt, "Interference model for back-focal-plane displacement detection in optical tweezers," Opt. Lett. **23**(1), 7–9 (1998).
24. http://cismm.cs.unc.edu/resources/software-manuals/video-spot-tracker-manual/
25. A. van der Horst and N. R. Forde, "Power spectral analysis for optical trap stiffness calibration from high-speed camera position detection with limited bandwidth," Opt. Express **18**(8), 7670–7677 (2010).
26. P. Mangeol, T. Bizebard, C. Chiaruttini, M. Dreyfus, M. Springer, and U. Bockelmann, "Probing ribosomal protein-RNA interactions with an external force," Proc. Natl. Acad. Sci. U.S.A. **108**(45), 18272–18276 (2011).
27. M. C. Noom, B. van den Broek, J. van Mameren, and G. J. L. Wuite, "Visualizing single DNA-bound proteins using DNA as a scanning probe," Nat. Methods **4**(12), 1031–1036 (2007).
28. R. T. Dame, M. C. Noom, and G. J. L. Wuite, "Bacterial chromatin organization by H-NS protein unravelled using dual DNA manipulation," Nature **444**(7117), 387–390 (2006).
29. E. Ronzitti, M. Guillon, V. de Sars, and V. Emiliani, "LCOS nematic SLM characterization and modeling for diffraction efficiency optimization, zero and ghost orders suppression," Opt. Express **20**(16), 17843–17855 (2012).
30. A. Farré, F. Marsà, and M. Montes-Usategui, "Optimized back-focal-plane interferometry directly measures forces of optically trapped particles," Opt. Express **20**(11), 12270–12291 (2012).
31. A. Farré and M. Montes-Usategui, "A force detection technique for single-beam optical traps based on direct measurement of light momentum changes," Opt. Express **18**(11), 11955–11968 (2010).
32. S. B. Smith, Y. Cui, and C. Bustamante, "Overstretching B-DNA: the elastic response of individual double-stranded and single-stranded DNA molecules," Science **271**(5250), 795–799 (1996).
33. P. Mangeol and U. Bockelmann, "Interference and crosstalk in double optical tweezers using a single laser source," Rev. Sci. Instrum. **79**(8), 083103 (2008).
34. C. López-Quesada, J. Andilla, and E. Martín-Badosa, "Correction of aberration in holographic optical tweezers using a Shack-Hartmann sensor," Appl. Opt. **48**(6), 1084–1090 (2009).
35. E.-L. Florin, A. Pralle, E. H. K. Stelzer, and J. K. H. Hörber, "Photonic force microscope calibration by thermal noise analysis," Appl. Phys., A Mater. Sci. Process. **66**(7), S75–S78 (1998).
36. K. Berg-Sørensen and H. Flyvbjerg, "Power spectrum analysis for optical tweezers," Rev. Sci. Instrum. **75**(3), 594–612 (2004).
37. A. Rohrbach, "Stiffness of optical traps: quantitative agreement between experiment and electromagnetic theory," Phys. Rev. Lett. **95**(16), 168102 (2005).
38. E. R. Dufresne and D. G. Grier, "Optical tweezer array and optical substrates created with diffractive optics," Rev. Sci. Instrum. **69**(5), 1974–1977 (1998).
39. M. D. Wang, H. Yin, R. Landick, J. Gelles, and S. M. Block, "Stretching DNA with optical tweezers," Biophys. J. **72**(3), 1335–1346 (1997).
40. J. P. Rickgauer, D. N. Fuller, and D. E. Smith, "DNA as a metrology standard for length and force measurements with optical tweezers," Biophys. J. **91**(11), 4253–4257 (2006).
41. T. Odijk, "Stiff Chains and Filaments under Tension," Macromolecules **28**(20), 7016–7018 (1995).
42. J. van Mameren, P. Gross, G. Farge, P. Hooijman, M. Modesti, M. Falkenberg, G. J. L. Wuite, and E. J. G. Peterman, "Unraveling the structure of DNA during overstretching by using multicolor, single-molecule fluorescence imaging," Proc. Natl. Acad. Sci. U.S.A. **106**(43), 18231–18236 (2009).
43. E. Eriksson, S. Keen, J. Leach, M. Goksör, and M. J. Padgett, "The effect of external forces on discrete motion within holographic optical tweezers," Opt. Express **15**(26), 18268–18274 (2007).
44. G. M. Gibson, J. Leach, S. Keen, A. J. Wright, and M. J. Padgett, "Measuring the accuracy of particle position and force in optical tweezers using high-speed video microscopy," Opt. Express **16**(19), 14561–14570 (2008).
45. F. Czerwinski, "allan v1.71," MatlabCentral 21727 (2008), *http://www.mathworks.com/matlabcentral/fileexchange/21727*
46. D. W. Allan, "Statistics of atomic frequency standards," Proc. IEEE **54**(2), 221–230 (1966).

#198832 - $15.00 USD Received 4 Oct 2013; revised 19 Nov 2013; accepted 19 Nov 2013; published 3 Dec 2013

47. D. Preece, S. Keen, E. Botvinick, R. Bowman, M. Padgett, and J. Leach, "Independent polarisation control of multiple optical traps," Opt. Express **16**(20), 15897–15902 (2008).
48. I. Moreno, J. A. Davis, T. M. Hernandez, D. M. Cottrell, and D. Sand, "Complete polarization control of light from a liquid crystal spatial light modulator," Opt. Express **20**(1), 364–376 (2012).
49. F. Kenny, D. Lara, O. G. Rodríguez-Herrera, and C. Dainty, "Complete polarization and phase control for focus-shaping in high-NA microscopy," Opt. Express **20**(13), 14015–14029 (2012).
50. A. Arias, S. Etcheverry, P. Solano, J. P. Staforelli, M. J. Gallardo, H. Rubinsztein-Dunlop, and C. Saavedra, "Simultaneous rotation, orientation and displacement control of birefringent microparticles in holographic optical tweezers," Opt. Express **21**(1), 102–111 (2013).

1. Introduction

Multiple laser beams are increasingly required in many optical trapping experiments [1]. The reasons are diverse: to manipulate multiple objects or grab large samples from several sides, to create traps with sophisticated intensity profiles [2] or to use a dual-beam geometry (either for trapping and detection or for detection alone) to reduce low-frequency instabilities [3–5], among others.

Acousto-optic deflectors (AODs) [6] or galvano-mirrors [7] are the preferred methods for steering the laser beam in two dimensions. However, they show limitations for creating multiple traps by scanning one single laser through different positions (time-sharing), since the refreshing takes place at a limited frequency, which can produce significant position fluctuations [8].

The other common technology is based upon spatial light modulators (SLMs) [9]. Unlike time-shared optical traps, holographic optical tweezers (HOTs) are permanent. In addition, axial control of the trapping sites is possible and sophisticated light patterns can also be generated. Since the first use of HOTs in the late 1990s, this technique has become increasingly popular for the dynamic manipulation of multiple samples [2, 10]. However, up to now its use in position and force measurements has been rather limited.

A number of authors have analyzed the characteristics and performance of holographic traps for quantitative experiments. In [11], it was shown that the potential wells of holographic traps were harmonic within a range of a few hundred nanometers, and in [12] the associated stiffness was found to vary by only 4% over a range of 20 μm across the sample plane. Large forces have also been measured with HOTs [13], in which the overstretching transition of double-stranded DNA (dsDNA) at 65 pN was used as a ruler. The position stability of stationary traps was found to be similar to non-holographic systems in the frequency range of 10 - 10^4 Hz [14]. On the other hand, the minimum step size attainable with modulators was obtained theoretically and experimentally (~2 nm) [12, 15] and the intensity changes during trap steering, which is one of the distinctive drawbacks of HOTs, were thoroughly analyzed and minimized in [16, 17]. Algorithms for hologram calculation have been designed with very high efficiency (up to 99%) [18], and their implementation in real time is possible, with both CPUs [19, 20] and GPUs [21].

Nevertheless, as pointed out by Moffitt *et al.* [22], the resistance found to HOTs turning into a standard technique outside their own field of application is ultimately based on the lack of a method for measuring the displacements and forces exerted on the trapped samples "*that rivals the resolution and bandwidth offered by back-focal plane interferometry*" [22, 23]. The typical position resolution of this method is in the order of 1 nm or less, and the sampling frequency can reach some hundreds of kilohertzs. The main alternative, high-speed video tracking, which consists of monitoring the displacements of the sample by means of a video camera, cannot yet provide the same performance, especially regarding the temporal response, typically in the order of some kilohertzs for high-speed cameras. Position resolution can be brought down to less than 1 nm using especial analysis software (such as [24]), but the impossibility of determining relative displacements of the sample from the center of the trap complicates the force measurements. In addition, video tracking has some other important drawbacks, such as blurring [25], off-line calibration, or the generation of large data files.

Here, we present an optical trap design that combines the wide range of possibilities of HOTs for manipulation and the measurement of positions and forces through BFPI. First, we describe the system and analyze and discuss its properties. Then, we use it in a single-

#198832 - $15.00 USD Received 4 Oct 2013; revised 19 Nov 2013; accepted 19 Nov 2013; published 3 Dec 2013

molecule experiment to assess its performance and finally discuss the long-term stability of the proposed configuration.

2. Experimental design

Our optical trapping system is built on a commercial inverted microscope (Nikon TE2000-E). We use an infrared (1064 nm) Ytterbium fiber laser (IPG YLM-5-1064-LP) with linear polarization (see Fig. 1). The laser power at the sample is regulated by a half-wave plate (HWP) and a polarizing beam-splitter. A second HWP allows us to finally select the polarization of the beam illuminating the SLM (Hamamatsu X10468-03). The modulator shapes the beam so the propagation of the laser can be remotely controlled with a computer in order to create multiple traps at the sample or beams with special properties, among others. The laser is expanded with the L1-L2 telescope to slightly overfill the SLM active area (16x12 mm^2), and is reduced back with the L3-L4 telescope to fill the entrance pupil of the microscope objective used to generate the optical traps (Nikon water-immersion, 60x, NA = 1.2). The same lens is used to observe the trapped particles and determine their positions with a high-speed EMCCD camera (Andor iXon3-860).

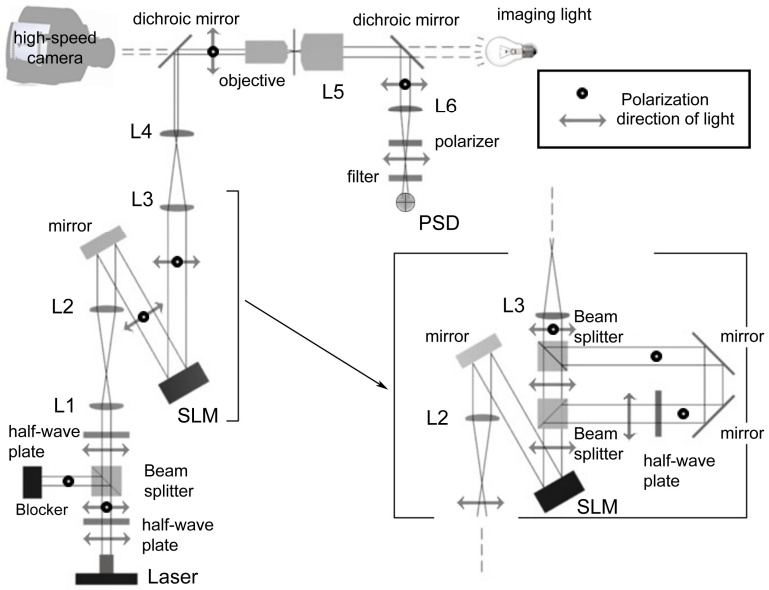

Fig. 1. Optical layout of our instrument. Alternatively (see Section 3.4), the setup could be reconfigured for comparison purposes, using additional optics (right-hand side) to split the beam by polarization. As a result, two traps with orthogonal polarizations were generated without resorting to the SLM.

The setup also includes a BFPI system for detection of positions and forces. However, the trapping laser cannot be used to detect the position of individual particles when several holographic traps are simultaneously active. In BFPI, the light from the trapping laser is scattered by the sample and collected by a lens (typically the illumination condenser of the microscope, L5 in Fig. 1). The light pattern at the back focal plane (BFP) of this lens is projected by means of an additional lens (L6) onto a position detector that finally provides a voltage proportional to the sample displacement and, eventually, to the optical force [23]. However, light from multiple traps in a conventional HOT system cannot be separated at the BFP of the collection lens, where all the scattered light merges into a single intensity pattern.

In general, a possible solution to discriminate the contribution from several traps is to label them using different polarizations and set a polarizer in front of the detector to isolate the light from one of them. Although only orthogonal polarizations can be used, the solution covers a wide range of multiple-trap experiments in which precise force measurements are

#198832 - $15.00 USD Received 4 Oct 2013; revised 19 Nov 2013; accepted 19 Nov 2013; published 3 Dec 2013

required [26–28]. In these experiments, a set of traps with a common linear polarization are used only for manipulation whereas an additional trap with crossed polarization is used for both manipulation and detection. We propose here a procedure by which an SLM easily generates these two sets of orthogonally polarized traps, making compatible the use of HOTs with BFP displacement detection.

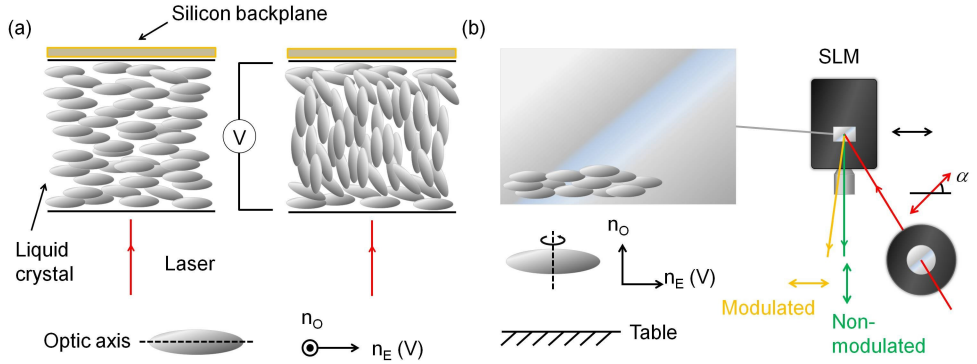

Fig. 2. (a) In the LC display, the molecules change their orientation when a voltage is applied to them. (b) For our SLM, the LC molecules tilt in a plane parallel to the optical table, which determines the direction of the extraordinary refractive index. The ordinary axis is perpendicular to it. When a linearly polarized beam oscillating with a certain angle, α, impinges on the LC, the phase of the component parallel to the table is controlled by the orientation of the molecules, since the effective refractive index of the material $n_E(V)$ depends on the voltage V through the tilt (this is the normal mode of operation). In contrast, any perpendicular component always sees the same refractive index, n_O, which is independent of the applied voltage. In consequence, after the SLM, the laser is split into two different beams: a pure holographic (modulated) and a pure non-holographic (unmodulated) beam.

Phase-only modulators commonly used in optical trapping are liquid crystal on silicon (LCoS) devices. They contain a cell full of a uniaxial nematic liquid crystal (LC) material. The LC is made of a viscous suspension of anisotropic molecules with an optic axis that defines two different refractive indexes in the medium: the (o)rdinary and the (e)xtraordinary (see Fig. 2(a)); while the extraordinary refractive index depends on the angle between the optic axis and the direction of light propagation, the ordinary refractive index is always the same. When a voltage is applied between the two faces of the cell, the orientation of the molecules changes and, with it, the optic axis. This causes a change in the extraordinary refractive index, n_E, while the ordinary index, n_O, remains constant. By varying the voltage, the effective optical length traveled by the light linearly polarized in the direction of the extraordinary axis can be controlled locally or, in other words, we can modulate the phase of the incoming wavefront. This corresponds to the normal operation of the device. However, light linearly polarized in the perpendicular direction travels through the LC cell with the ordinary refractive index, which is the same regardless of the orientation of the molecules. Any component of light with this polarization is reflected off the SLM, as in a mirror.

By using a linearly polarized laser oscillating at a certain angle (α) to the extraordinary axis, we generate two components labeled with orthogonal polarizations: a holographic term, modulated by the SLM, and a stationary non-holographic component located at the zero order (see Fig. 2(b)). A half-wave plate (HWP) in front of the SLM is used to regulate the ratio of laser powers between these two components. Light modulated by the SLM can still steer the beam three-dimensionally to create one trap or to generate multiple traps or other patterns for complex manipulation. The laser, after impinging on the SLM, is focused by the microscope objective and creates two sets of traps with perpendicular polarizations. After interacting with the samples, the laser is collected by the condenser lens. Now, the contribution from the centered, zero-order trap can be separated from the rest by means of a linear polarizer located in front of the photodetector, and BFPI can be used to measure the sample displacement in that trap. It should be emphasized that this zero-order trap is deliberately created by us with

#198832 - $15.00 USD Received 4 Oct 2013; revised 19 Nov 2013; accepted 19 Nov 2013; published 3 Dec 2013

crossed polarization and controlled intensity. It is, therefore, different from the unmodulated spot that arises due to the limited diffraction efficiency of the SLM, which is commonly filtered out or otherwise suppressed [29]. As this unmodulated spot of light has the same polarization as holographic traps, it cannot be used for measuring purposes.

Our system for BFP detection has been described in detail in [30]. In short, positions of the trapped bead are measured in the BFP of the illumination condenser of the microscope (Nikon, oil-immersion, NA = 1.4) with a position sensitive detector (PSD, Thorlabs, PDP90A) (see Fig. 3). A dichroic mirror deflects the infrared beam toward the PSD while keeping the illumination capabilities of the condenser. A relay lens group after the mirror images the light pattern at the BFP of the collecting lens onto the detector. A linear polarizer (analyzer) finally selects the desired polarization for detection.

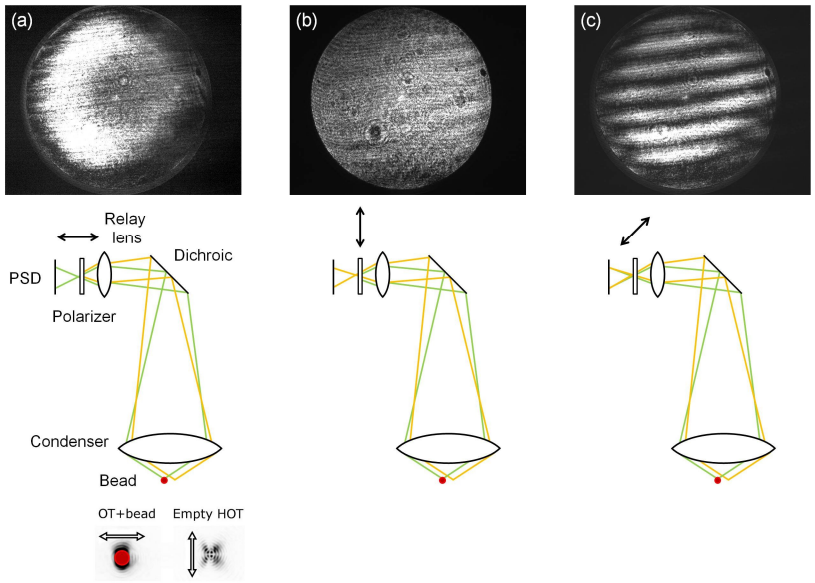

Fig. 3. Intensity patterns recorded at the BFP of the condenser with a conventional CCD camera. The bead is in the non-holographic trap (OT) and the holographic trap (HOT) is empty. Each column corresponds to a different angle of the analyzer: (a) parallel to the non-holographic beam, (b) parallel to the holographic (empty) beam and (c) at 45°. Hollow arrows indicate the polarization of the traps and the solid arrow the orientation of the analyzer.

In a two-trap setup, we can easily observe at the BFP that the information on each trap is available by choosing the corresponding polarization. For example, when the transmission axis of the analyzer is set parallel to the polarization of the non-holographic trap, which is holding a bead, and we leave the holographic beam empty, a typical BFP circular interference pattern shows up [31] (see Fig. 3(a)). In contrast, if the analyzer is set perpendicularly (see Fig. 3(b)), the BFP pattern corresponds to that of the laser alone, as expected (a uniform disk). This indicates that the two traps have rather pure polarizations and can be effectively separated. Any intermediate angle shows typical Young interference fringes (see Fig. 3(c)) arising from the superposition of the two traps' projections. Similar results are obtained when the microsphere is held in the holographic trap.

In our setup, the position measurements are carried out with the non-holographic trap, since only one detector is available. This beam is static as it is not modulated by the SLM: it cannot be moved during the experiments. The remaining traps display typical HOT functionality and can be modulated as usual. An alternative configuration that we have not yet tested is to use the non-modulated, ordinary light beam for detection only, reducing its power and creating a holographic trap at the same position for manipulation. This solution is akin to that used in some experiments where an auxiliary, weaker laser spot with a different wavelength is used to interrogate the sample position [4].

#198832 - $15.00 USD Received 4 Oct 2013; revised 19 Nov 2013; accepted 19 Nov 2013; published 3 Dec 2013

DNA preparation protocol

We carried out a DNA-stretching experiment for testing the instrument (Section 3.3). The purification of DNA, its labeling with biotin and digoxigenin and the coating of the beads with streptavidin (SA) and anti-digoxigenin (AD) are explained elsewhere [13]. The DNA, at a concentration of 0.7 nM, was incubated for one hour with the AD beads (2.1 μm) at room temperature before each experiment. The ratio of DNA molecules per bead was set to 80 DNA / bead to improve the frequency of DNA tethering. Finally, the beads were incubated with 12 mg/ml bovine serum albumin (BSA) for 20 minutes to block non-specific interactions during the experiment, and were washed a couple of times to remove the unbound BSA. Likewise, the flow chamber was incubated at the same BSA concentration for 20 minutes to avoid undesired interactions between the beads and the glass walls.

Experiments were performed in a commercial flow chamber (Warner Instruments RC-30WA) filled with a specific buffer solution (150 mM NaCl, 10 mM Tris and 1 mM EDTA, pH 8.0) to observe the DNA overstretching at 65 pN [32].

3. Analysis of the system

In this section, we first analyze the crosstalk between traps for a number of holographic spots. Then, we explore the effect of optical aberrations of the non-modulated beam on trapping efficiency. For comparison with previous results [13], we use the system to stretch single dsDNA molecules, and, finally, we explore the stability of the differential signal between two traps at low frequencies.

3.1 Crosstalk

In common holographic schemes, all traps have the same polarization, corresponding to the extraordinary axis of the birefringent LC molecules. When the laser beams are collected by the condenser lens, light comes together at the BFP and amalgamates into a complex pattern caused by the multiple beam interferences. The intensity distribution no longer provides information about the position of individual objects. In our system, the use of the extra, non-modulated trap with crossed polarization avoids contamination of the detector reading by spurious light from the other holographic traps. However, as found by [33], some depolarization can be observed for large angles (corresponding to the periphery of the light patterns) and gives a certain crosstalk level. In our instrument, we recorded the PSD voltage from an empty non-holographic trap when a 1.87-μm bead fixed to the coverslip was scanned across the holographic trap (see arrow in Fig. 4(a), red curve), and found the maximum to be 0.5% of the position signal obtained when the bead was moved across the non-holographic trap instead (see Fig. 4(a), black curve). As crosstalk depends on the relative laser power between the two polarizations, when several holographic traps were created, crosstalk was found proportional to the number of extra traps (see Fig. 4(a), inset).

#198832 - $15.00 USD Received 4 Oct 2013; revised 19 Nov 2013; accepted 19 Nov 2013; published 3 Dec 2013

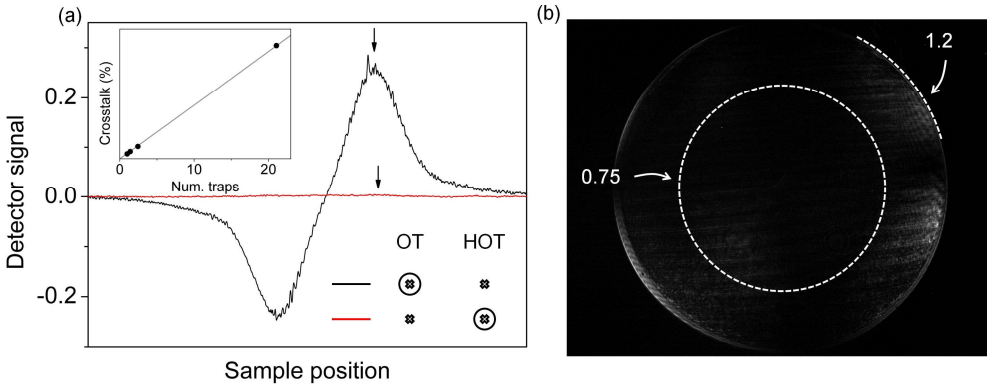

Fig. 4. Analysis of the crosstalk between traps. (a) BFPI signal when the analyzer is set to record the non-holographic light that we use for position detection, and the bead is first moved across this non-holographic (OT) trap (black curve) and then across the holographic (HOT) one (red curve). The level of crosstalk is proportional to the number of traps (inset). (b) The BFP pattern of an empty trap when the analyzer selects the complementary polarization is an almost constant dark disk with NA = 1.2, which corresponds to the NA of the trapping objective (the acceptance angle of the condenser extends further to NA = 1.4). The pattern shows the effect of depolarization, mainly at large angles, close to the edges. If the effective NA of the condenser is reduced from 1.4 to 0.7-0.8 using an iris (dotted circle), the crosstalk decreases drastically as the amount of depolarized light within this region is insignificant. This improves the position signal and was the configuration used for the experiment.

In the experiment, we limited the numerical aperture of the condenser lens used to collect the light scattered by the sample to an effective value of about 0.75 (using an iris placed at its BFP), which is sufficient for accurate BFPI position measurements. The effective NA of the collecting lens when the iris was used was determined by calibrating the BFP to convert positions to NA as detailed in [31] (see Fig. 4(b)). Depolarization takes place more strongly at large angles and shows up at the BFP of the collecting lens as a cross-shaped pattern with four bright lobes at the edges [33]. With a 1.4-NA condenser, when the whole BFP pattern was projected onto the detector, crosstalk increased from 0.5% to >3% per extra trap and was no longer a negligible effect. Therefore, especially if our system is used with several holographic traps or if the non-holographic term is generated with relatively low laser power, it is advisable to limit the numerical aperture of the condenser.

On the other hand, the presence of unmodulated light coming from the limited efficiency of the SLM (typically a small fraction of the total laser power) does not alter the position measurements, despite that this light interacts with the sample. This effect is already taken into account in the bead displacement calibration as long as it remains more or less constant.

3.2 Trap harmonicity

We calibrated the traps through the analysis of the thermal motion of trapped samples to determine the potential well created by the light, especially in the non-holographic focus (see Fig. 5). The bead used for calibration was 1.87 μm in diameter and the laser power at the sample was 40 mW. This trap was not corrected for the aberrations introduced by the SLM, so, in principle, astigmatism or spherical aberration induced by the back-plane of the device could degrade the linear relation between force and position or could even make the trapping impossible [34].

#198832 - $15.00 USD Received 4 Oct 2013; revised 19 Nov 2013; accepted 19 Nov 2013; published 3 Dec 2013

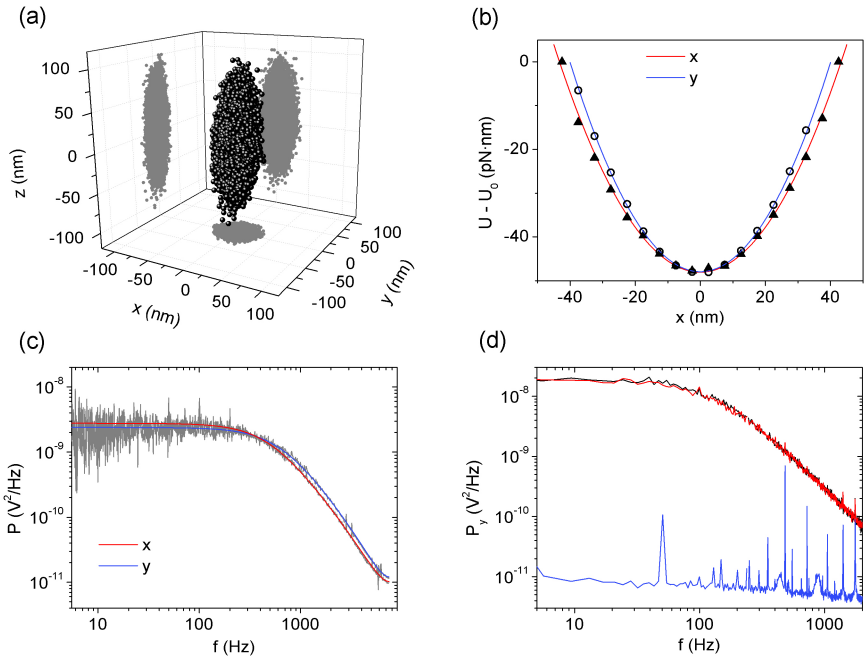

Fig. 5. (a) Volume of the positions visited by a 1.87-μm microsphere trapped in the non-holographic trap, during calibration. (b) The confining potential is reconstructed from the probability distribution of positions, $U = -k_B T \ln(p)$ [35]. The fluctuations of the particle are compatible with a harmonic potential within a range of at least 50 nm, the range of thermally-driven displacements during calibration. (c) Power spectrum data of the Brownian motion and fitting. The roll-off frequency takes the values f_c = 477 Hz and f_c = 602 Hz in x and y, respectively. (d) Power spectra of the non-holographic component, in the presence of an empty (red) or filled (black) holographic trap. If the bead in the non-holographic trap is released, the power spectrum of the laser alone is obtained (blue). The same behavior was observed when the holographic polarization was chosen instead.

Astigmatism typically shows up as a decrease in trap stiffness, especially in the axial direction, and as a strong radial asymmetry of the intensity profile, which translates into clearly different values of k_x and k_y. We found, however, no significant differences in the distribution of positions of the trapped particle along x and y for our SLM (see Fig. 5(b)). Furthermore, the reconstructed potential followed a perfect parabola, $U = ½ (k_x x^2 + k_y y^2)$. We also found a good agreement between the experimental power spectra and the predicted theory when different calibration effects were taken into account [36], obtaining similar spring constants in the two directions (see Fig. 5(c)), k_x = 1.21 ± 0.09 pN/μm·mW and k_y = 1.52 ± 0.11 pN/μm·mW, and in consonance with the reported values for non-aberrated traps [37]. As expected, we obtained less stiffness in the axial direction, k_z = 0.35 ± 0.03 pN/μm·mW, since it is always the weaker axis [37], but there were no notable differences with the transverse components. This indicates both small astigmatism and spherical aberration.

The holographic trap also showed harmonic behavior within the range of positions that the sample visited during calibration. In addition, the power spectrum for each polarization did not seem affected by the presence of an extra trap with perpendicular polarization, indicating low crosstalk between measurements (see Fig. 5(d)).

We tested the quality of the non-modulated trap in an optical setup that uses a different SLM of the same series (Hamamatsu X10468-03). We found similar results in trapping stability; and the manipulation of microspheres did not seem to be compromised by the aberrations of this second modulator, either. The nominal optical flatness of this device was worse, but by examining the shape of the non-modulated spot in the alignment procedure

#198832 - $15.00 USD Received 4 Oct 2013; revised 19 Nov 2013; accepted 19 Nov 2013; published 3 Dec 2013

during the construction of the setup, we managed to compensate the aberrations of the SLM with other optical elements. When aberrations make the trapping with the non-modulated spot difficult, one could always add a static correction hologram, similar to those used in [38]. Another possibility is to add to the set of holographic traps another corrected, modulated trap at the zero order for manipulation, and to use light of the non-holographic component for position detection only.

3.3 Experiment: DNA stretching

The system was further analyzed through an experiment consisting in stretching dsDNA molecules [39]. In particular, we examined the effect of SLM aberrations at high forces and the mutual interference between traps. The use of DNA as a metrology standard has been demonstrated in previous studies, which followed different strategies with satisfactory results [13, 40]. The well-known elastic properties of this molecule provide a perfect test bench for an optical trapping system.

Single 11.7-kbp-long molecules labeled with biotin and digoxigenin were attached by their ends to two different microspheres (coated with streptavidin and anti-digoxigenin, respectively) and were stretched as the force and separation of the two ends were recorded. Two types of beads with different sizes (2.1 μm and 3.17 μm) were used in the experiments in order to visually identify the labels. We used the large spheres to monitor the force with the non-holographic trap, and the small beads were held in the steered beam. Steps of different sizes were used along the curve (100 nm and 20 nm), so that it was more densely sampled for separations of the beads close to the contour length of the molecule (L_c = 3.96 μm). The laser power of the non-holographic trap was around 110 mW and the recording frequency 15 kHz.

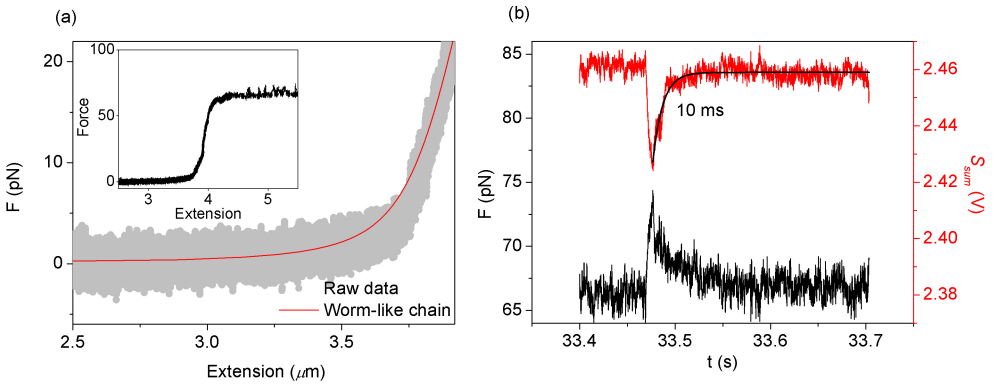

Fig. 6. (a) DNA stretching curve. The data fitted Odijk's formula for low forces (< 20 pN). From the fitting, we obtained L_c = 4.02 μm, L_p = 41 nm and K = 690 pN. (b) Correlation between the spikes at high forces and the intensity drops due to the "dead time" during the update of the hologram.

Figure 6(a) shows the results of the DNA stretching experiment. For low forces (<20 pN), the force-extension curve complies with Odijk's formula [39, 41]. In our experiments, L_c, the persistence length, L_p, and the elastic modulus, K, were taken as free parameters. The results (L_c = 4.02 μm, L_p = 41 nm and K = 690 pN) were in good agreement with previously reported values [39]. When the molecule is further stretched beyond L_c, the backbone undergoes a structural transition due to the conversion from double-stranded to single-stranded DNA [42], and the characteristic overstretching plateau [32] shows up (see Fig. 6(a), inset). The high forces achieved in this experiment indicate that the aberrations of the SLM backplane are not significant enough to degrade the non-holographic trap performance.

The separation of the two beams into orthogonal polarizations overcomes some issues observed in a prior holographic experiment. As our dumbbell did not show crosstalk between traps, no modulations were observed in the force, as opposed to the results in [13]. In contrast,

#198832 - $15.00 USD Received 4 Oct 2013; revised 19 Nov 2013; accepted 19 Nov 2013; published 3 Dec 2013

we observed noisier traces at high forces. Oscillations of 1 pN, similar to those observed in [42], were seen. Although they are comparable to those reported in [13], we believe that they have different origins since no such modulations were observed at low forces. We also observed peaks at high forces, which seemed to be caused by the hologram update. The HOT response is ultimately limited by the refreshing rate of the modulator. During this "dead time" the SLM is not correctly modulating the beam and the intensity at the sample drops. If an external force is being applied, the bead is pulled away for a short period of time (tens of milliseconds) [43] before the hologram is displayed back on the LC (see Fig. 6(b)).

3.4 Long-term stability

Among the possibilities that multiple-beam systems offer, the dumbbell configuration has emerged in recent years as a promising advance that pushes the position resolution of optical traps down to the subnanometer level by reducing low-frequency noise. Different strategies have been put forward for enhancing long-term stability. In 2004, Nugent-Glandorff and Perkins [3] used an auxiliary beam as a fiducial mark to eliminate the drift introduced by the microscope stage. Abbondanzieri *et al.*, following a different approach [4], suspended the sample in a dual-trap system to eliminate the drift and filled the laser path with helium. In combination with a force-clamp, they achieved a resolution in position better than 1 Å. With a similar configuration, Moffitt *et al.* reduced the difference in path length between the two laser beams and used the correlations from the two trapped samples to reduce the long-term noise to a similar level [5].

In all these experiments, the most common option to build the dual-beam system was to divide the laser by means of polarization [4, 5]. The use of electro-optic devices to create the multiple beams, such as AODs or SLMs, is usually avoided since they can introduce additional sources of noise.

However, systems based on these technologies presumably share a large long-term stability of the differential position between traps due to an inherent common optical path design. For example, two optical traps generated by an SLM can be thought of as encoded into a single complex wavefront that divides into two foci only after being focused by the objective, with essentially zero optical path difference between them. A difference in the optical path length which is nominally zero should lead to a perfect constant separation between traps regardless of environmental conditions. This property has been barely explored likely due to the existence of other important limitations: in the time-shared approach, the oscillations introduced by the limited refresh time of the laser when scanned through all the traps and, in HOTs, the lack of a method comparable to BFPI to measure positions and forces, among others.

The stability of the differential signal of two holographic traps was analyzed in [44]. Following a similar procedure, we explore here the difference in stability between a dual-trap system constructed using two different methods: separating the laser by polarization and using our trapping scheme. We recorded the motion of two trapped beads (2.19 μm) with a high-speed camera at 2 kHz to explore the long-term stability in both cases.

In our holographic dumbbell, the instability of the position over a 75-s measurement decreased from 15 nm to 2 nm peak-to-peak when we analyzed the differential signal instead of the single traps separately (see Fig. 7). These results are comparable to those with more sophisticated designs, although no special experimental requirements were needed in our case. We used the Allan variance [45] of the series to obtain greater insight into the long-term stability of the system. This technique has been widely used to analyze the stability of atomic clocks [46].

Brownian noise dominates the sample motion only for high frequencies. Other sources of noise, such as air currents or microscope drifts, dominate below 10 Hz, giving a deviation of ~2 nm for the 75-s measurements. This result would lead to large errors if the second bead was stuck to the coverslip or held by a micropipette. However, when the position of this trap is compared with the position of its twin trap, we observed that the Allan variance is much smaller, reaching a minimum value of 0.24 nm.

#198832 - $15.00 USD Received 4 Oct 2013; revised 19 Nov 2013; accepted 19 Nov 2013; published 3 Dec 2013

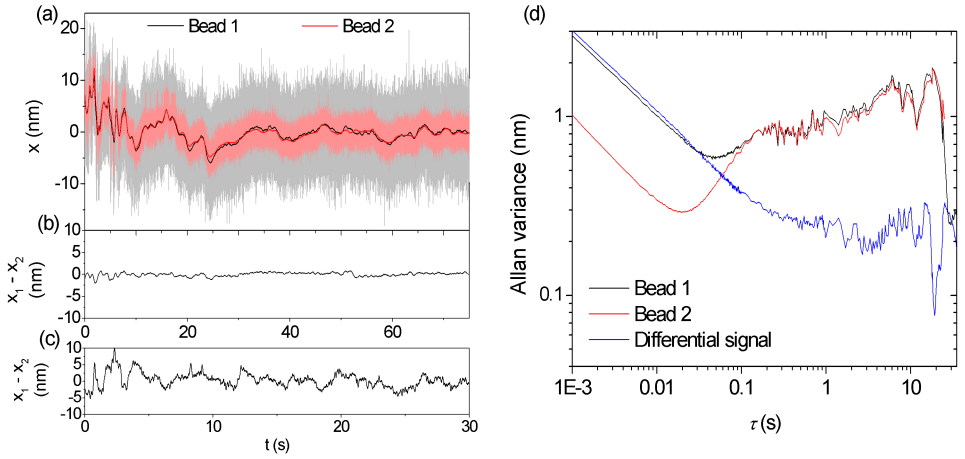

Fig. 7. (a) Positions of beads 1 (black curve) and 2 (red curve) extracted from a 75-s movie. Light and dark colors correspond to raw and filtered data, respectively. (b) Distance between the particles shown in (a) with our holographic design and (c) with two independent traps obtained by the division of a single laser. (d) Allan variance of the three signals of the HOT setup.

When we compare the stability results with those obtained with the dumbbell built by physically splitting the laser into two beams and rotating 90° the polarization of one of them (experimental layout on the right-hand side of Fig. 1), we observe that the distance between beads shows greater fluctuation under similar conditions (see Fig. 7(c)). Low-frequency noise increases from 2 nm peak-to-peak to more than 10 nm. Although we tried to make the system as compact as possible, this is due to the difference in the optical paths now followed by the two lasers. Mechanical disturbances, such as vibrations of the optical elements or air currents, affected the two beams in different ways and gave rise to small differences in the positions of the traps.

4. Discussion and conclusions

HOTs have been scarcely used in precise force measurement experiments. The use of high-speed cameras [25, 44] has been accepted as adequate for particle tracking and force determination when more than one trap is in use. However, at present, BFPI is still notoriously superior regarding spatial and temporal bandwidths. In this study, we propose to utilize non-modulated light propagating through the ordinary SLM axis for the generation of a fixed trap with perpendicular polarization with respect to the set of dynamic, holographic traps. Light from the extra trap can be isolated from the rest with little crosstalk and be used for BFP interferometric position detection.

Although we have discussed how several useful experimental geometries can be implemented through this approach, our setup is nevertheless somewhat rigid, as force measurements can only be done on one of the traps, which is furthermore necessarily static.

The creation of traps or patterns with arbitrary polarizations was demonstrated elsewhere [47–50] for other purposes. In theory, those systems would allow selection of any of the holographic traps and the taking of BFPI measurements at any site, in the presence of other traps designed with orthogonal polarizations. Therefore, problems derived from aberrations in the non-modulated, zero-order trap, for example, would be avoided easily. However, the experimental setups providing such flexibility are more complex than ours. They involve employment of two modulators [49], a single modulator in a double-pass scheme [48, 50] or one in a split-screen configuration [47], at the expense of increasing costs or reducing spatial resolution. In addition, since very precise pixel-to-pixel alignment is required and stability is plausibly worsened, they are not necessarily suitable for the kind of applications that we have discussed.

#198832 - $15.00 USD Received 4 Oct 2013; revised 19 Nov 2013; accepted 19 Nov 2013; published 3 Dec 2013

The solution proposed in this study is very simple, both conceptually and experimentally, as it uses the same setup and algorithms of common HOTs. We achieved nanometer long-term stability with a pair of traps that had crossed polarizations. We also successfully applied and measured large forces in a single molecule-stretching experiment to demonstrate the performance of our system.

Acknowledgments

We are grateful to N. R. Forde, M. Shayegan and N. Rezaei for providing us with the DNA samples and to J. Martínez, who started the project. This research has been partly funded by the Spanish Ministry of Education and Science (FIS2010-16104), the Government of Catalonia–ACC1Ó (VALTEC G614828324059231) and the Barcelona Knowledge Campus Initiative (FPC2010-17). A. F. acknowledges an FI grant from the Generalitat de Catalunya (Government of Catalonia).

#198832 - $15.00 USD Received 4 Oct 2013; revised 19 Nov 2013; accepted 19 Nov 2013; published 3 Dec 2013